

# Precipitant-Controlled Growth of Lysozyme Crystals in Sodium Thiocyanate

Wayne F. Jones, Mark A. Arnold, and John M. Wiencek\*

*Chemical and Biochemical Engineering, University of Iowa, 4122 Seamans Center, Iowa City, Iowa 52242*

*Received July 14, 2003; Revised Manuscript Received August 23, 2004*

**ABSTRACT:** We have shown previously that large high-quality single protein crystals can be grown by varying temperature in a predetermined fashion such that the solution supersaturation and the rate of crystal growth are maintained at a constant value in batch crystallization systems. Here we have adapted the constant supersaturation control (CSC) methodology to isothermal crystal growth. In this version of the CSC protocol, dynamic control is provided by changing precipitant concentration through a dialysis membrane. We have developed a system of multiple growth cells in series that allows a variety of precipitant concentration trajectories to be sampled simultaneously during a single CSC experiment. Several different concentration profiles were used to grow lysozyme crystals in NaSCN salt. Increasing the precipitant concentration using a slow linear profile results in the highest quality crystals while requiring the least amount of characterization work. Coupling this type of profile with multiple growth cells in series appears to be a promising method for dynamically controlling protein crystal growth isothermally.

## Introduction

Protein structure determination using X-ray diffraction (XRD) requires a single crystal, or crystals, of the candidate protein. Generally, a protein crystal suitable for XRD should be large ( $>0.1$  mm in all dimensions) and have a high degree of internal order. That is, the three-dimensional crystal lattice must be ordered, regular, and free of defects. The growth of suitable crystals is often the most difficult and time-consuming step in the structure determination process. We have grown large, high-quality crystals using temperature to control protein solubility with constant supersaturation control (CSC) algorithms.<sup>1,2</sup> CSC algorithms change temperature in a predetermined fashion such that the solution supersaturation and the rate of crystal growth are maintained at a constant (slow) rate.

However, not every protein/solvent system displays a temperature-dependent solubility.<sup>3</sup> To be a truly general method, the CSC protocol must therefore be applicable to proteins that do not display solubility that is temperature dependent. Additionally, since most protein screens generate initial candidate crystals isothermally there is an obvious need to extend the CSC approach to isothermal crystal growth. In this incarnation of the CSC protocol, protein solubility control is provided by changing the precipitant concentration, in a predetermined fashion, throughout the course of an experiment.

The precipitant control approach is applied to the lysozyme/NaSCN system. This system was chosen for two main reasons. First, it is a fairly difficult to grow diffraction quality crystals in this system. Figure 1 shows an example of batch lysozyme crystals grown in 0.12 M NaSCN. The crystals are of poor quality, composite, and are unsuitable for X-ray diffraction. Second, we have extensive experience applying temperature control algorithms to this system. The application of temperature control results in significant improvements over batch crystallization.<sup>2</sup> This background

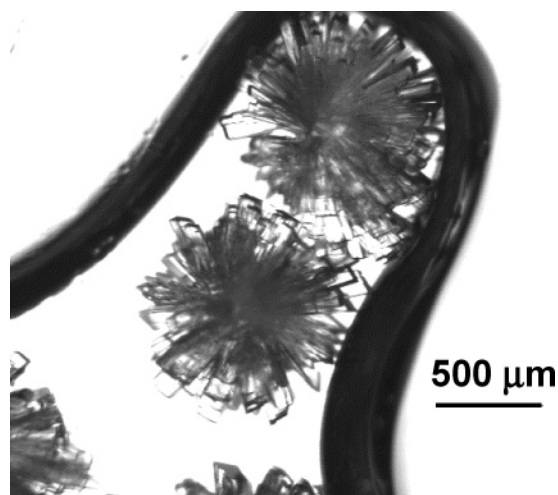


**Figure 1.** Typical image of a batch lysozyme crystals grown in NaSCN. These composite crystals were grown at 18 °C in 0.12 M NaSCN, 50 mM acetate buffer, pH 4.5.

allows us to readily adapt the temperature algorithms to precipitant algorithms and facilitates direct comparison of the resulting crystals to the batch and temperature control crystals.

The study described in this manuscript is preliminary in nature and is meant to explore the feasibility of the precipitant control methods discussed. As such, crystal quality assessments are based on overall size and morphology (i.e., optical clarity and lack of defects) as opposed to actual X-ray data. However, crystal size and optical clarity provide a reasonable initial estimate of X-ray diffraction quality for this system as we have shown in a prior publication.<sup>2</sup>

**Precipitant-Controlled Growth.** The CSC predictive algorithm is a mass balance that incorporates crystal growth rate information.<sup>1,2,4</sup> The growth rate is controlled by a given variable—typically, a thermodynamic variable—such as temperature, protein concentration, or precipitant concentration. For the isothermal

protocols discussed here, precipitant concentration is used to control protein solubility and therefore nucleation and growth. Crystal growth rate information coupled with the initial state of the system is sufficient to calculate the trajectory of the system (i.e., crystal growth as a function of time). Obtaining a simple mathematical growth rate expression is key to the CSC approach. The growth rate is typically expressed as a function of supersaturation. Thus, any growth rate model incorporates the solubility of the protein into its expression, in addition to any kinetic constants. This work utilizes a simple rate expression so that it can be widely utilized without extensive characterization work. Temperature-based CSC algorithms benefit greatly from a single calorimetric experiment which provides accurate growth rate and solubility information, as a function of temperature. However, systems that do not display a temperature-dependent solubility will, as clearly indicated by the van't Hoff relationship, have a heat of crystallization that is essentially zero, thus precluding calorimetric evaluation of a growth rate expression.

To easily adapt the temperature control protocols to precipitant control, some simplifying assumptions are made about the system. First, it is assumed that slow growth rates are advantageous and lead to improved crystal quality.<sup>2,5</sup> The microgravity environment of space often dramatically decreases the rate of growth of crystals, and many investigators conjecture that this slow, diffusion-limited growth rate is the primary reason for improved quality in space grown crystals.<sup>6–8</sup> In mass transfer limited growth we can assume a simple film model for the mass transfer<sup>9</sup>:

$$\frac{dm}{dt} = k_f A (C - C_{\text{sat}}) \quad (1)$$

where  $m$  is the mass of the crystal,  $k_f$  is the film coefficient,  $A$  is the surface area of the crystal,  $C$  is the concentration of protein in the liquid phase, and  $C_{\text{sat}}$  is the solubility of the protein under the particular thermodynamic conditions of the system at that moment in time. The mass and surface area of the crystal can be related to its size ( $L$ ) via the crystal density ( $\rho = \text{mass of protein per volume of crystal}$ ), volume shape factor ( $k_V = 8$  for a cube), and area shape factor ( $k_A = 24$  for a cube):

$$m = \rho k_V L^3 \quad (2)$$

$$A = k_A L^2 \quad (3)$$

Using these definitions and eq 1, the growth rate expression ( $G$ ) can be related to the film model expression for a cube:

$$G = \frac{dL}{dt} = k_f \frac{(C - C_{\text{sat}})}{\rho} \quad (4)$$

Using the approach that proved successful in temperature-based CSC, it is assumed that only one crystal will form during the experiment resulting in a simple mass balance on the system:

mass of protein in liquid initially (no crystals) = mass of protein in single crystal at time ( $t$ ) + mass of protein

remaining in liquid at time ( $t$ ) or

$$V_{\text{soln}} C_0 = \rho k_V L^3 + V_{\text{soln}} C \quad (5)$$

In eq 5,  $V_{\text{soln}}$  is the volume of the crystallizing solution,  $C_0$  is the initial protein concentration in the crystallizing solution, and  $C$  is the protein concentration at a given time.

The CSC approach assumes that the supersaturation remains constant, which fixes  $G$  to a constant value ( $G_0$ ). Further,  $L$  can be calculated at any time,  $t$ , by integrating eq 4 to yield  $L = L_0 + G_0 t$ .<sup>1</sup> For an unseeded experiment,  $L_0 = 0$  (thus,  $L = G_0 t$ ).  $C$  and  $C_{\text{sat}}$  must change in time in a manner consistent with maintaining  $G$  at a constant value of  $G_0$ .  $C_{\text{sat}}$  is the controlled variable and will be moderated to satisfy this requirement by changes in the precipitant concentration. Thus, removing the variable  $C$  from the resulting expression by combining eqs 4 and 5 yields:

$$C_{\text{sat}} = C - \rho \frac{G_0}{k_f} = C_0 - \rho k_V \frac{L^3}{V_{\text{soln}}} - \rho \frac{G_0}{k_f} = C_0 - \rho k_V \frac{(G_0 t)^3}{V_{\text{soln}}} - \rho \frac{G_0}{k_f} \quad (6)$$

Notice the final form of this equation is entirely predictive.  $C_0$ ,  $G_0$ ,  $V_{\text{soln}}$  are fixed by the experimentalist;  $\rho$ ,  $k_V$ ,  $k_f$  are physical constants of the system. The one kinetic constant, a mass transfer film constant ( $k_f$ ), can be estimated from the proteins diffusion coefficient ( $D$ ) and the film thickness ( $\Lambda$ ):

$$k_f \approx \frac{D}{\Lambda} \quad (7)$$

It is a reasonable approximation to set the film thickness,  $\Lambda$ , equal to the edge-to-edge length of the final crystal, which can be estimated from the mass balance (eq 5) based on the anticipated final concentration of the protein in solution.

This simple mass transfer model allows one to directly predict how best to modify the protein's solubility as a function of time. The only remaining step is to relate the solubility to a given precipitant concentration. In principle, this mapping can be obtained using static light scattering (SLS) to measure  $B_{22}$  as a function of the precipitant concentration.<sup>10</sup> In addition, dynamic light scattering can be used to directly measure the diffusion coefficient ( $D$ ) of a protein in a particular system. This study uses published data to estimate solubility as a function of precipitant concentration<sup>11</sup> and published diffusion coefficients.<sup>12</sup>

The values of  $C_0$ ,  $G_0$ ,  $V_{\text{soln}}$ ,  $\rho$ ,  $k_V$  are identical to those used for temperature-controlled growth and are reported by Jones et al.<sup>2</sup> Equation 5 and the final protein concentration from the corresponding temperature control experiment provide an estimate of  $\Lambda = 370$  microns. Using the reported diffusivity of lysozyme<sup>12</sup> ( $1.1 \times 10^{-6}$  cm<sup>2</sup>/s),  $k_f$  is estimated as  $2.96 \times 10^{-5}$  cm/s. Figure 2 shows lysozyme solubility as a function of time for a precipitant control experiment using the calculated mass transfer film coefficient. The lysozyme solubility shown in Figure 2 is identical to the solubility as a function of time for the corresponding temperature

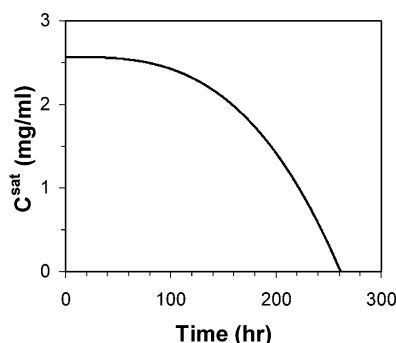


**Figure 2.** Lysozyme solubility as a function of time as predicted by a mass transfer limited growth rate model. This  $C_{\text{sat}}$  vs  $t$  curve is identical to the one actually employed in the corresponding lysozyme/NaSCN temperature control experiment.

control experiment. The  $C_{\text{sat}}$  versus time curve shown is then translated into an isothermal precipitant concentration versus time curve as discussed above. The resulting precipitant-based CSC profile is shown graphically in the results and discussion section.

Note that the above crystal growth rate expression (eq 4) assumes that the crystal growth rate is limited by diffusion of protein to the growing crystal. Clearly, at sufficiently high supersaturation this assumption will fail. However, the first assumption of this model is that slow growth is the desired outcome. Thus, if growth is too fast and not diffusion-limited, the experimentally fixed initial supersaturation should be reduced. Provided the initial supersaturation is sufficiently small the assumption of diffusion-limited growth will be correct.

### Experimental Methods

Microdialysis buttons immersed in a flow through cell were utilized to implement the isothermal growth profile. Crystal nucleation and growth are achieved by increasing the precipitate concentration of the cell solution surrounding the dialysis button. The solubility of the protein inside the button decreases as precipitant inside the button equilibrates with the exterior cell solution by diffusion across the dialysis membrane. The rate of diffusion of water or other small molecular weight buffer constituents through the dialysis membrane material is a relatively slow process with an approximate first-order decay having a half-life of 10 h.<sup>13</sup> The precipitant profiles shown in this paper incorporate the lag time for mass transfer across the dialysis membrane using a half-life of 10 h. However, this correction is insignificant for these experiments, which is not surprising since the lag of 10 h is an order of magnitude smaller than the experimental duration of 200 plus hours.

**Lysozyme Preparation.** A stock solution of hen egg white lysozyme (Sigma lot 51K7028) was dialyzed at 4 °C for 2 days against deionized water, and then for 2 days against 50 mM acetate buffer pH 4.6, using a 3500 molecular weight cutoff (MWCO) membrane (Spectra/Por). Lysozyme solutions of approximately 3.0 mg/mL were prepared in 0.1 M NaSCN and 50 mM acetate buffer and loaded into 50  $\mu$ L dialysis buttons (Hampton Research HR3–326). The buttons were covered with 3500 MWCO dialysis membranes (Spectra/Por). Lysozyme concentrations were determined by UV spectrophotometer at 280 nm using an extinction coefficient of 26.35 (10 mg/mL solution, 1-cm path length). All solutions were passed through 0.2  $\mu$ m syringe filters prior to sample preparation.

**Experimental Apparatus.** We have adapted a preparative scale liquid chromatography (LC) pump and computer-controlled gradient former (Foxy Jr., ISCO) to experimentally control precipitant concentration. A software program was

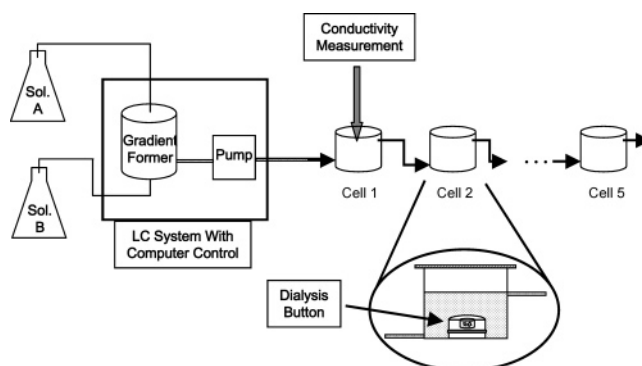


**Figure 3.** Apparatus used for precipitant-controlled growth experiments. The LC pump and gradient former were computer controlled to automatically pump a desired precipitant concentration and volume into the apparatus. The apparatus consisted of five growth cells in series. The volume of each cell was about 20 mL. The concentrations of the NaSCN stock solutions were nominally 0.1 M NaSCN (solution a) and 0.2 M NaSCN (solutions b). NaSCN concentrations were measured using conductivity.

written to periodically pump the desired concentration and volume of precipitating solution into the flow through cell apparatus. In this case the flow through apparatus consists of five cells connected in series rather than just a single flow through cell (Figure 3). The cells were constructed of screw top plastic scintillation vials. Each cell had a nominal working volume of 20 mL. The vials were connected in series via HPLC tubing and fittings and sealed against leakage using rubber gasket material. This system of cells in series allows one to easily screen multiple, in this case five, precipitant concentration trajectories in a single experiment. This is advantageous not only because it simplifies and streamlines the experimental process by allowing one to run five experiments simultaneously but also because it accounts for the inherent variability of the crystallization process. Many variables can significantly effect the outcome of a given crystallization experiment. For example, precipitant concentration, protein concentration, temperature, and pH all impact the size and quality of crystals produced. As mentioned previously the rate of nucleation and growth are also important variables in the crystallization process. The uncertainty associated with all of these variables can result in radically different outcomes of even two identical crystallization experiments. Additionally, the precipitant profiles utilized in these experiments are calculated based on published solubility data and incorporate certain assumptions (for example, formation and growth of a single crystal) that may not be completely accurate. Arranging the precipitant cells in series allows for the sampling of several precipitant concentration trajectories surrounding the calculated profile. Further, having the ability to sample multiple precipitant concentration trajectories, and therefore crystal growth trajectories, reduces the amount of characterization work required. This method allows an experimentalist to rationally approach a crystallization experiment with minimal knowledge of the crystallization behavior of a given protein.

**Salt Concentration.** For this set of experiments lysozyme crystals were grown at room temperature (approximately 20  $\pm$  1 °C) using NaSCN salt as a precipitating agent. On the basis of the calculated precipitant profile NaSCN concentration was generally varied between 0.1 and 0.2 M during the course of a crystallization experiment. Experimentally the LC pump and gradient former performed most accurately when solutions A and B, shown in Figure 3, had NaSCN concentrations that were nominally 0.1 M (solution A) and 0.2 M (solution B). Precipitant concentration was measured using an Orion temperature compensated conductivity meter and probe (meter: 135A, conductivity cell: 011010A). Measured conductivity readings were converted to molar NaSCN concentrations using a linear correlation ( $r^2 = 0.998$ ). The correlation was deter-

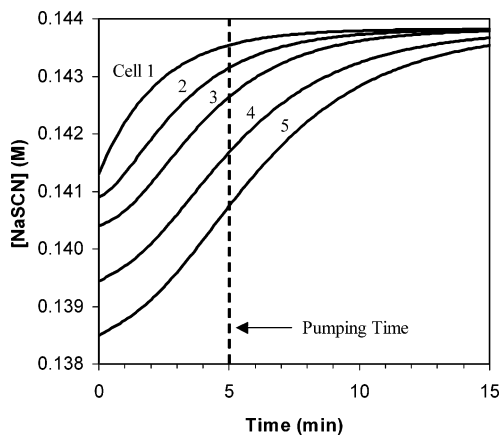


**Figure 4.** Example unsteady-state concentration profiles for each cell. The profiles were calculated using eq 8 fitted to the tracer data. The five minute pumping time used for all experiments is also shown on the figure.

mined by measuring the conductivity of six standard solutions from 0.1 to 0.2 M NaSCN.

**Growth Cells in Series.** Conductivity is a simple, accurate, and high-resolution method of monitoring salt concentration during a precipitant-controlled growth experiment. However, because commercially available probes are generally large relative to the size of our growth cells ( $\sim 20$  mL volume), and the potential for disruption of the growing crystals inside the cells, we were unable to monitor each individual cell during the experiment. Therefore, the flow characteristics were modeled using an unsteady-state mole balance for each of the cells in series.<sup>14</sup> Solving the differential equation for each cell results in the general equation shown below:

$$C_n = C_{n,0} \exp\left[\frac{-t}{\alpha_n \tau_n}\right] + C_{(n-1)} \left(1 - \exp\left[\frac{-t}{\alpha_n \tau_n}\right]\right) \quad (8)$$

where  $C_n$  is the concentration of NaSCN in cell ( $n$ ) after pumping into the cell for time ( $t$ ), ( $C_{n,0}$ ) is the initial NaSCN concentration in cell  $n$ , ( $\tau_n$ ) is the space time of cell  $n$ , ( $C_{(n-1)}$ ) is the concentration in cell ( $n-1$ ). Tracer data using NaSCN was collected to validate this model.  $\alpha_n$  is an adjustable parameter for cell  $n$  used to fit the tracer data to eq 8. Note that for  $n = 1$ ,  $C_{(n-1)}$  is equal to the NaSCN concentration pumped into the system.

Tracer experiments were performed by pumping a known concentration of NaSCN into the apparatus for 5 min, and measuring the resulting conductivity of each cell. Figure 4 shows an arbitrary example of the unsteady-state concentration profile in each cell for a typical step increase in NaSCN concentration. The concentration profiles were calculated using eq 8 fitted to the tracer data. The figure suggests that by pumping for 5 min cell 1 reaches the target concentration of NaSCN while maintaining a reasonable range of concentration in the remaining growth cells. This suggestion was verified by experiments in which NaSCN concentration was measured after 5 min of pumping time.

The adjustable parameter ( $\alpha_n$ ) was used to regress an apparent space-time ( $\alpha_n \tau_n$  in eq 8) of each cell using the measured NaSCN concentrations from the tracer experiment. Table 1 summarizes the results of the tracer studies and regression for each of the five cells. The table shows the nominal working volume ( $V_n$ ), the volumetric flow rate ( $v_n$ ), the adjustable parameter ( $\alpha_n$ ), the apparent volume ( $V_{a,n} = \alpha_n V_n$ ), and the resulting apparent space time ( $\tau_{a,n} = V_{a,n}/v$ ) for each cell.

The model, with regressed space-times, was then used to predict the NaSCN concentration of an independent data set. Using this method we found that we could predict the NaSCN

concentration in each cell to about 1% error ( $0.7 \pm 0.39\%$ ), which is approximately the error of the conductivity measurement.

For the crystal growth experiments described below the NaSCN concentration was calculated in each of the five cells. All cells were initially filled with identical concentrations of NaSCN by pumping a target concentration of NaSCN for 30 to 40 min. A step increase in NaSCN concentration was then pumped into the apparatus for 5 min. The initial concentration in each of the five cells was then measured using conductivity. At this point 50  $\mu$ L dialysis buttons were prepared and placed in the apparatus as discussed above. For the remainder of the experiment, programmed stepwise increases of NaSCN were initiated using the computer-controlled apparatus based on the calculated precipitant profiles discussed previously. For each step, the desired NaSCN concentration was pumped into the apparatus for five minutes at a rate of 8.8 mL/min. After 5 min the pumping was stopped and the system was allowed to relax while NaSCN equilibrated across the dialysis buttons containing the crystallization solution. The length of time that pumping was stopped depends on the experimental profile being implemented (see Results and Discussion). The concentration of NaSCN in each cell was calculated after each step increase using the initially measured NaSCN concentrations, regressed  $\alpha_n$  values, and eq 8. Crystal images were captured after removal of the dialysis buttons at the conclusion of the experiment. NaSCN concentration was also measured via conductivity at this time. Final conductivity measurements verified the 1% accuracy of the calculated NaSCN concentrations.

## Results and Discussion

On the basis of the procedure outlined above three different examples of experimental precipitant control profiles are discussed. The three experiments explore different approaches to precipitant-controlled growth. The first experiment closely follows the CSC precipitant control profile. The other two experiments are more empirical in nature. The empirical experiments are derived from the CSC profile and use linear increases in precipitant concentration. Experiments using linear profiles were performed to determine if a simplified approach could be used to obtain high-quality crystals in a system that has not been extensively characterized.

Figure 5 shows an example of a crystal growth experiment. For this experiment, 3.21 mg/mL lysozyme was prepared as discussed in Experimental Methods. The lysozyme solution was pipetted into 50  $\mu$ L dialysis buttons, and the buttons were placed in the growth cells of the apparatus. As shown in the figure, the NaSCN concentration was increased stepwise using the CSC profile as a guide. The smooth curve in the center shows the CSC profile calculated based on eqs 1–7. The lines bracketing the CSC concentration profile are the NaSCN concentrations actually implemented in this experiment. For clarity, Figure 5 shows only the NaSCN concentrations in cells 1 (top line) and 5 (bottom line). Also, the figure only shows NaSCN concentrations up to about 0.14 M. The experimental NaSCN concentration for this experiment was increased to approximately 0.18 M, but the concentrations above 0.14 M are omitted because they are difficult to see clearly on the figure.

Although the difference in NaSCN concentration in cell 1 (top line) and cell 5 (bottom line) may appear small, the difference in the crystallization environment from cell to cell is significant. This is most easily seen by examining the percent relative supersaturation (eq 9) of the crystallizing solutions at the start of the

**Table 1. Nominal Cell Volumes ( $V_n$ ), Volumetric Flow Rate ( $v_n$ ), Regressed  $\alpha_n$  Values and Corresponding Apparent Cell Volume ( $V_{a,n}$ ) and Apparent Space-Time ( $\tau_{a,n}$ )<sup>a</sup>**

cell 1	cell 2	cell 3	cell 4	cell 5
$V_1$ (mL) = 20.00	$V_2$ (mL) = 20.00	$V_3$ (mL) = 20.00	$V_4$ (mL) = 20.00	$V_5$ (mL) = 20.00
$v_1$ (mL/min) = 8.80	$v_2$ (mL/min) = 8.80	$v_3$ (mL/min) = 8.80	$v_4$ (mL/min) = 8.80	$v_5$ (mL/min) = 8.80
$\alpha_1$ = 1.00	$\alpha_2$ = 1.18	$\alpha_3$ = 1.30	$\alpha_4$ = 1.83	$\alpha_5$ = 1.80
$V_{a,1}$ (mL) = 20.00	$V_{a,2}$ (mL) = 23.55	$V_{a,3}$ (mL) = 26.03	$V_{a,4}$ (mL) = 36.56	$V_{a,5}$ (mL) = 35.94
$\tau_{a,1}$ (min) = 2.27	$\tau_{a,2}$ (min) = 2.68	$\tau_{a,3}$ (min) = 2.96	$\tau_{a,4}$ (min) = 4.15	$\tau_{a,5}$ (min) = 4.08

<sup>a</sup> Values were determined by regression of tracer experiments.

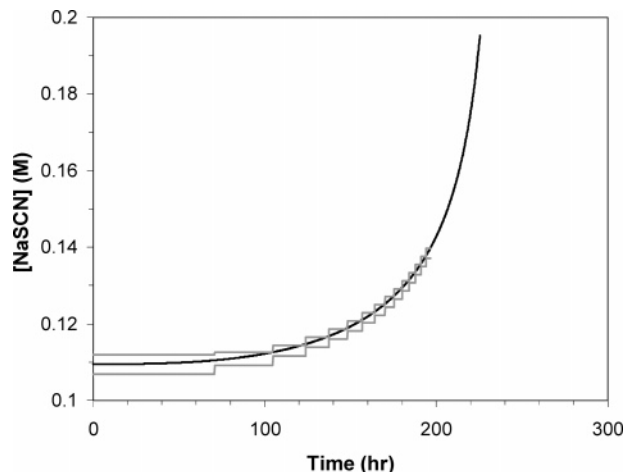


**Figure 5.** CSC NaSCN concentration profile (smooth curve) shown with the actual NaSCN concentrations implemented during the experiment. Implemented NaSCN concentrations are shown for cells 1 (top line) and cell 5 (bottom line) only.

experiment ( $t = 0$  in Figure 5). Using eq 9 with the

$$\frac{(C - C_{\text{sat}})}{C_{\text{sat}}} \times 100 \quad (9)$$

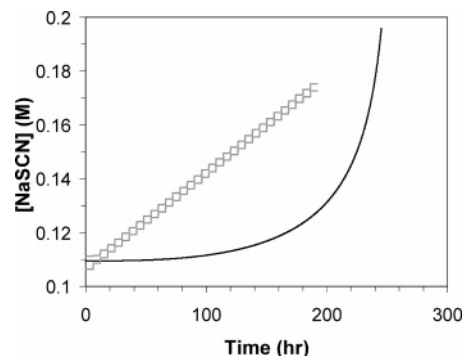
measured protein concentration given above (3.21 mg/mL) and the literature solubility<sup>11</sup> (at the measured initial salt concentration) gives a percent relative supersaturation (PRS) of 27% for cell 1 and 12% for cell 5. The 15% difference between cells 1 and 5 is seen to be particularly significant in light of the fact that the change in PRS of any given cell over the duration of the entire experiment ( $t = 223$  h) is approximately 62%.

Figure 6 shows an image of the lysozyme crystals grown using this concentration profile. The image is of crystals from cell 3 taken at the conclusion of the experiment (223 h). The crystals in the image are reasonably well formed, about 100–200  $\mu\text{m}$  in size, and are a significant improvement over batch lysozyme crystals grown in NaSCN (Figure 1). However, the large number of crystals suggests that nucleation occurred when the NaSCN concentration was increasing rapidly (i.e., high on the smooth curve in Figure 5). Thus, nuclei were initiated under conditions of rapidly increasing supersaturation, promoting further nucleation and rapid growth of the many nuclei already formed. That this system would nucleate at higher NaSCN concentration than desired is not surprising considering its sensitivity and some of the assumptions used in calculating the profile.

As stated previously, it is our goal to keep the crystallization protocols as simple and usable as possible. With this goal in mind, experiments in which the



**Figure 6.** Example image of lysozyme crystals grown using the stepwise NaSCN concentration profile shown in Figure 5. The image was taken from a dialysis button in cell 3 at the conclusion of the experiment (223 h). The crystallizing solution consisted of 3.21 mg/mL lysozyme in 50 mM acetate buffer pH 4.6 at approximately 20 °C.



**Figure 7.** In this example, the implemented linear stepwise profile is based on the starting and ending points of the CSC profile (smooth curve) shown in the figure. The NaSCN concentration is shown in cell 1 (top line) and cell 5 (bottom line) only. NaSCN concentration was increased by 2.1 mM every 6 h.

precipitant concentration was increased linearly were also conducted. Figure 7 shows an experiment using a linear increase in NaSCN concentration. In this case, the linear profile is derived from the starting and ending points of the CSC profile. The resulting increase in NaSCN concentration is 2.1 mM every 6 h. Again the stepwise experimental concentrations shown are for cells 1 and 5 only. For this experiment, the initial lysozyme concentration was 3.16 mg/mL, resulting in an initial PRS of 24% for cell 1 and 9% for cell 5.

Figure 8 shows an image of a lysozyme crystal grown using this profile. The image is of a crystal taken from cell 4 at the conclusion of the experiment (192 h). The crystal is fairly large (450  $\mu\text{m}$ ) and appears well formed.

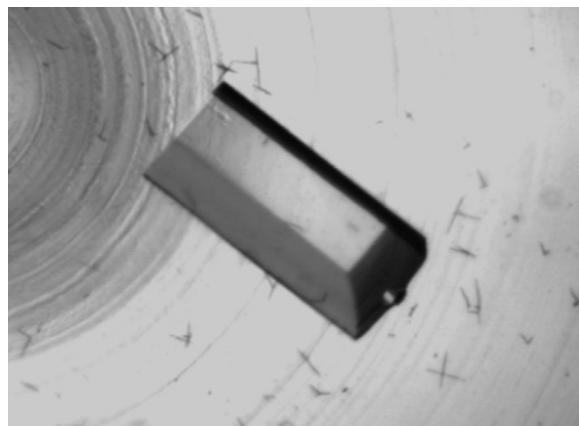


**Figure 8.** Example image of a lysozyme crystal grown using the linear NaSCN concentration profile shown in Figure 7. The image was taken from a dialysis button in cell 4 at the conclusion of the experiment (192 h). The crystallizing solution consisted of 3.16 mg/mL lysozyme in 50 mM acetate buffer pH 4.6 at approximately 20 °C.

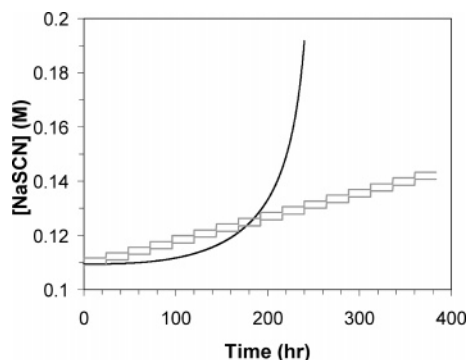


**Figure 9.** In this example, the implemented stepwise profile is based on a “slow” linear increase in the NaSCN concentration. The start of the implemented profile corresponds to the start of the CSC profile (smooth curve) shown in the figure. The NaSCN concentration is shown in cell 1 (top line) and cell 5 (bottom line) only. NaSCN concentration was increased by 2.1 mM every 24 h.

Figure 9 shows a “slow” linear stepwise increase in NaSCN concentration for cells 1 and 5. This empirical profile exploits the idea that a slow increase in precipitant concentration, and therefore slow crystal growth, will result in high-quality crystals. The slow linear profile results in a NaSCN concentration increase of 2.1 mM every 24 h. As shown in Figure 9, the starting point of the stepwise increase is based on the CSC profile. The initial lysozyme concentration was 3.17 mg/mL, resulting in a PRS of 25% for cell 1 and 12% for cell 5.

Figure 10 shows an image of a 530  $\mu\text{m}$  lysozyme crystal grown using this profile. The image is of a crystal from cell 3 and was taken at the conclusion of the experiment (384 h). In general, crystals grown using a slow linear profile appear to be larger and of superior optical clarity compared to those grown with one of the other profiles (Figures 5 and 7). This result supports the contention that slow, dynamically controlled growth results in crystals of higher quality.

The crystals shown in all three of the precipitant control profiles discussed here are superior to batch crystals such as those shown in Figure 1. Also, based on overall crystal size, optical clarity, and consistency

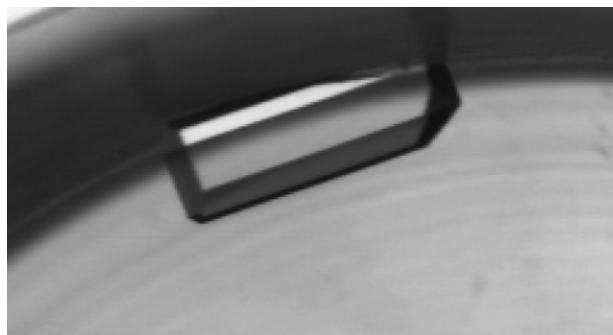


**Figure 10.** Example image of a lysozyme crystal grown using the linear NaSCN concentration profile shown in Figure 9. The image was taken from a dialysis button in cell 3 at the conclusion of the experiment (384 h). The crystallizing solution consisted of 3.16 mg/mL lysozyme in 50 mM acetate buffer pH 4.6 at approximately 20 °C.

of results, temperature control appears to be a superior approach for this particular system.<sup>2</sup> However, a definitive comparison of crystal quality between these two methods would require the direct comparison of X-ray data collected on crystals from each method.

Arranging crystal growth cells in series and subjecting each cell to distinct precipitant concentration profiles should result in differences in the number and quality of crystals grown in a given experiment. In fact, we do see definite qualitative differences in crystals from cell to cell. For example, the crystals produced by the precipitant profile shown in Figure 10 follow a pattern that may be expected for this particular experiment. The dialysis buttons in cells 1 and 2 contained a shower of tiny crystals, suggesting that the precipitant concentration in these cells was increased too rapidly, resulting in many nuclei and therefore many small crystals. The dialysis buttons in cell 3 contained about 10 crystals. All crystals in this button were small (<100  $\mu\text{m}$ ) except one large well-formed crystal in each button, including the crystal shown in Figure 10. The buttons in cell 4 contained 20–30 crystals. Most of the crystals in this cell were in the 300–400  $\mu\text{m}$  range. Several of the crystals appeared to be fairly well formed, while many showed obvious defects such as cracked or composite crystals. Finally, the buttons in cell 5 contained about 30 crystals. Some of these crystals were up to 600  $\mu\text{m}$  long but nearly all had defects. These results, while qualitative, suggest that there is an optimal precipitant-controlled crystallization trajectory for a given system, and that this trajectory can be sampled by using growth cells in series. Note that using a more sophisticated pump and gradient former the precipitant concentration step size could be decreased, resulting in a closer approximation of a desired precipitant concentration profile. Furthermore, by increasing the number of growth cells it is possible to sample a larger number of crystal growth trajectories. Sampling a larger number of trajectories would allow higher resolution screening over a small range of crystallization conditions or screening a wider range of conditions if the crystallization system is relatively uncharacterized.

We have used a CSC approach when calculating the precipitant control protocols discussed in this paper. However, when significantly deviating from this profile as shown in Figures 7 and 9 it is unlikely that the

crystal growth rate ( $G$ ) is constant. We view this as a reasonable trade off between extensive characterization work and ease of use of the method. Furthermore, implementing the precipitant-induced method using growth cells in series allows for sampling a variety of growth trajectories increasing the likelihood that an optimal, or near optimal trajectory is achieved.

### Conclusions

We have used an isothermal CSC protocol to grow what appear to be large, high-quality crystals of lysozyme using NaSCN as a precipitating agent. The lysozyme/NaSCN system was chosen as a test case for this method to allow for direct comparison to temperature-controlled growth profiles that we have used extensively in the past.<sup>2</sup> In terms of the size and overall quality of the crystals produced, temperature control appears to be superior for this system. However, as stated previously, not all protein systems display a temperature-dependent solubility. In such cases, precipitant-induced isothermal growth is a suitable extension of the CSC protocol. Increasing the precipitant concentration using a slow linear profile (Figure 9) appears to result in high-quality crystals while requiring the least amount of characterization work. Furthermore, using crystal growth chambers in series is a simple and useful method of screening multiple precipitant concentration trajectories. Coupling a slow linear precipitant profile with multiple chambers in series appears to be a promising method for dynamically growing protein crystals isothermally.

**Acknowledgment.** This work was supported by a grant from the National Aeronautics & Space Administration (Grant Number NAG8-1835).

### References

- (1) Schall, C. A.; Riley, J. S.; Li, E.; Arnold, E.; Wiencek, J. M., *J. Cryst. Growth* **1996**, *165*, 299–307.
- (2) Jones, W. F.; Wiencek, J. M.; Darcy, P. A. *J. Cryst. Growth* **2001**, *232*, 221–228.
- (3) Christopher, G. K.; Phipps, A. G.; Gray, R. J. *J. Cryst. Growth* **1998**, *191*, 820–826.
- (4) Darcy, P. A.; Wiencek, J. M. *Acta Crystallogr.* **1998**, *D54*, 1387–1394.
- (5) Garcia-Ruiz, J. M.; Moreno, A. *J. Cryst. Growth* **1997**, *178*, 393–401.
- (6) Koszelak, S.; Day, J.; Leja, C.; Cudney, R.; McPherson, A. *Biophys. J.* **1995**, *69*, 13–19.
- (7) Gerbi, D. J.; Egbert, W. C.; Ender, D. A.; Leung, P. C. W.; Rochford, K. B.; Virden, J. W. *J. Cryst. Growth* **1986**, *76*, 673–680.
- (8) McPherson, A. *J. Phys. D. Appl. Phys.* **1993**, *26*.
- (9) Cussler, E. L. *Diffusion, Mass Transfer in Fluid Systems*; Cambridge New York: Cambridge University Press, 1984.
- (10) Guo, B.; Kao, S.; McDonald, H.; Asanov, A.; Combs, L. L.; Wilson, W. W. *J. Cryst. Growth* **1999**, *196*, 424.
- (11) Guilloteau, J.; Ries-Kautt, M.; Ducruix, A. *J. Cryst. Growth* **1992**, *122*, 223–230.
- (12) Muschol, M.; Rosenberger, F. *J. Chem. Phys.* **1995**, *103*, 10424.
- (13) Lee, C. Y.; Sportiello, M. G.; Cape, S. P.; Ferree, S.; Todd, P.; Kundrot, C. E.; Lietzke, S.; Barnes, C. *Biotechnol. Prog.* **1997**, *13*, 77.
- (14) Fogler, H. S. *Elements of Chemical Reaction Engineering*, 3rd ed.; Prentice Hall: New Jersey, 1999; pp 10, 198.

CG0341297